Crack growth monitoring by strain measurements

KAMAYA Masayuki

Institute of Nuclear Safety System, Inc., 64 Sata, Mihama-cho, Fukui 919-1205 Japan (kamaya@inss.co.jp)

Abstract: Cracks detected during in-service inspections are not always removed when they are judged as hazardous. It is important to monitor the crack growth in order to secure the integrity of the cracked components. The author and a co-worker proposed a crack growth monitoring method, in which the elastic strain caused by internal pressure is continuously measured. The elastic strain acting at the outside surface of a pressurized pipe changes due to growth of a crack in the inside surface, and the magnitude of its change depends on the growth size. In this study, the author uses multiple strain gages to monitor the elastic strain acting on the cracked part of a pipe. An axial crack was introduced at the butt welding portion inside a carbon steel pipe. The strains were then measured under static internal pressure. The crack size was estimated based on the change in strains measured by strain gages attached onto the outside surface of the pipe. This study reveals that such a monitoring procedure could successfully identify not only the crack depth but also the surface length. The maximum estimation errors were 2.2 **mm** and 0.97 **mm** for the surface length and depth, respectively. The accuracy of the estimation improved as the number of strain gages increased. It was also apparent that the residual stress had subtle effect on the size estimation, albeit it may have significant influence when the crack propagates.

Keyword: crack size monitoring; elastic strain; surface crack; internal pressure

1 Introduction

If a crack is detected in nuclear power plant components during in-service inspections, the structural integrity of the cracked components is assessed by predicting the crack growth during futures operation. According to the fitness-for-service codes [1, 2], the detected cracks do not incessantly have to be repaired if the predicted crack size is sufficiently small. The size of the unrepaired crack is re-examined in the next outage in order to validate the growth prediction (shown in Fig.1). Ultrasonic testing (UT) is, in principle, generally used to identify the crack size when a crack is located inside a pipe. However, the accuracy of size identification using UT is reported to be more than a few millimeters [3], which is not good enough to capture the crack growth. Furthermore, in order to secure the component integrity, unknown factors in the growth prediction must be considered for safety. In view of this, the growth prediction tends to be excessively conservative.

With the aim to improve the accuracy of crack size identification and to exclude the conservativeness in the growth prediction, the author and a co-worker [4] proposed a crack growth monitoring method. By identifying the change in crack size, it is possible to verify the accuracy of the prediction.

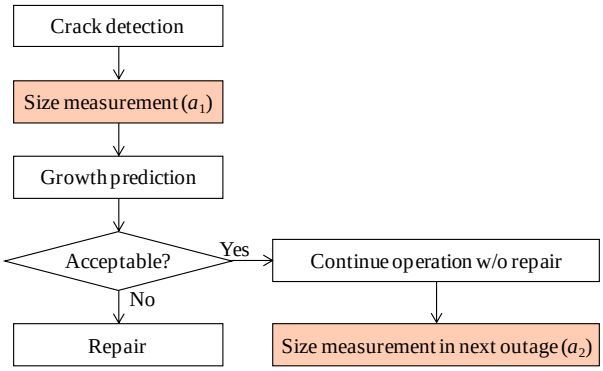

Fig. 1 Procedure for structural integrity assessment after crack detection.

In this monitoring method, the elastic strain caused by the internal pressure is measured during the plant operation. The strain at the outside surface of a pressurized pipe is changed due to a crack existing in the inside surface and the magnitude of its change depends on the size of the crack. By evaluating in advance the change in strain due to the crack by finite element analysis (FEA), it is possible to estimate the crack size. Since this method focuses on monitoring of an existing crack, the location and initial crack size

Received date: July 24, 2012
(Revised date: September 7,2012)

are identified at the initial stages of the monitoring. Strain gages are therefore applicable for strain measurements, making it possible to monitor the precise change in crack size during plant operation.

In another study conducted by the author and the same co-worker [5], feasibility of the monitoring method was shown by comparing results of the FEAs and experiments under static internal pressure of cracked pipes which had various machined notches of different geometry. The current study aims at improving the method. By using multiple strain gages attached at different positions and directions (axial or hoop strain), not only the crack depth but also the surface length could be estimated [6] and the accuracy of the crack size estimation was improved by taking the average of the estimated crack sizes obtained using multiple strain gages.

In the present paper, after a brief review of the basis of the monitoring method, a detailed procedure using multiple strain gages is presented. An experiment using a cracked pipe is thereafter described. An axial crack was introduced at the butt welding portion inside a carbon steel pipe. Since, in nuclear power plants, stress corrosion cracks have been initiated by welding residual stress, it is important to investigate the influence of the residual stress on the monitoring. The change in strains was measured by applying an internal pressure and the crack size was estimated. Finally, the validity of this monitoring method for practical use is discussed.

2 Crack growth monitoring method

2.1 Basic procedure

Figure 2 shows a schematic of the crack growth monitoring system [5]. The strain acting on the outside surface (outside strain) of the cracked pipe is measured and recorded continuously during plant operation. When the plant operates, the strain increases due to elastic deformation caused by internal pressure. The outside strain near a crack is different from that acting at an uncracked portion as schematically shown in Fig. 3. In other words, the compliance of the cracked portion against the internal pressure is altered by the crack. Although the strain is changed not only by the crack growth but also by various factors such as variations in the pressure or temperature and offset strain due to gage error or creep deformation, these effects can be compensated by quoting the strain at the uncracked portion.

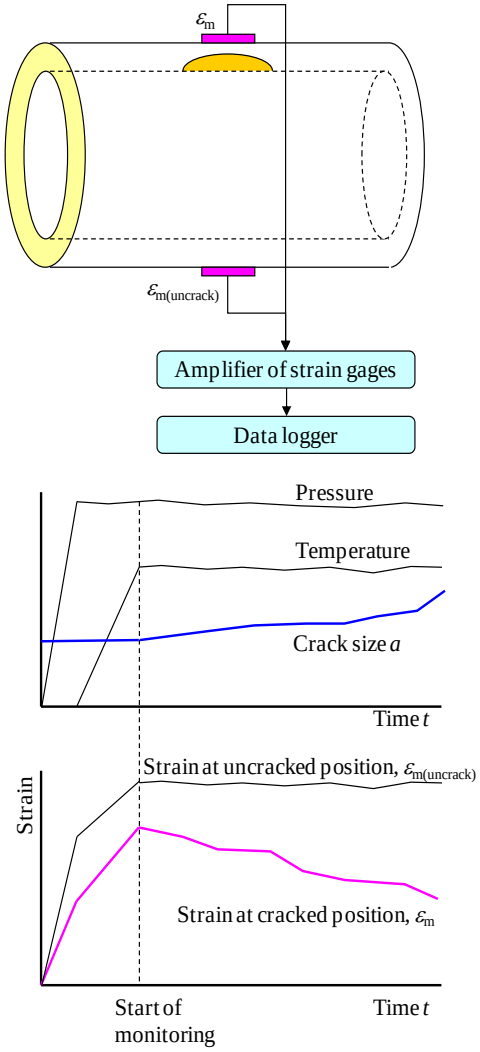

Fig. 2 Schematic of the monitoring method for the strain acting on the outside surface.

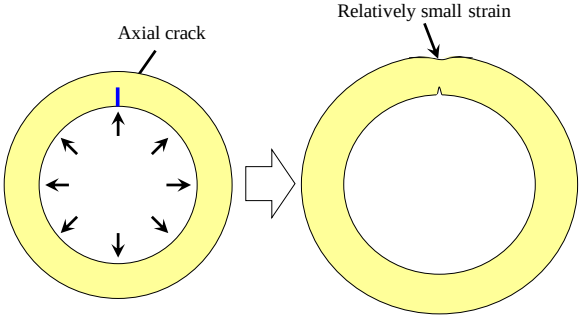

Fig. 3 Schematic representing the change in strain under internal pressure and the effect of internal cracking.

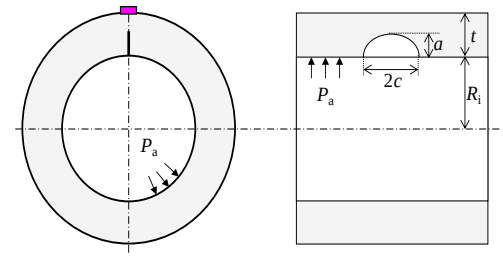

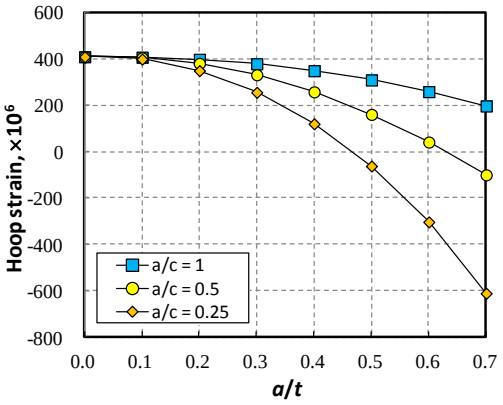

(a) Hoop strain

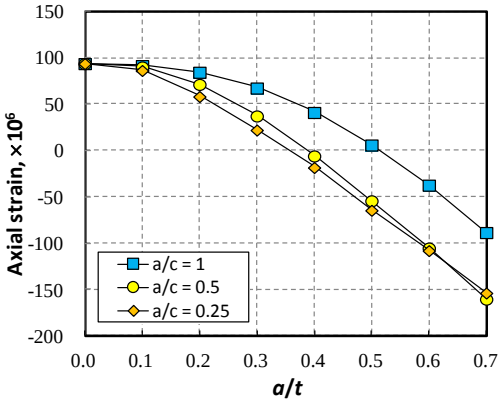

(b) Axial strain

Fig. 4 Change in outside strain with crack depth for various crack shapes (R_i = 128.8 **mm**, t = 17.1 **mm**, P_a = 30 **MPa**).

Figure 4 shows the FEA results for a cracked pipe under internal pressure. The change in strain with the crack depth (a) normalized by pipe thickness (t) was investigated under different values of the surface length ($2c$), which was normalized as aspect ratio (a/c). The detailed procedure and conditions of FEA are described in section 4 of this paper. The changes in the hoop and axial strains outside the pipe with crack depth were investigated. As is apparent in Fig. 4, the outside strain decreased as the crack size increased. The magnitude of the change was more than several hundred microstrains (με). Since accuracy of the strain measurement by strain gages is a few microstrains, it is possible to track small changes in the crack size. Additionally, the change in the strain also depended on the crack shape. A lower aspect ratio (a/c) caused a remarkably larger drop in the strain. Therefore, even if the crack shape is assumed to be semi-elliptical, the surface length has to be identified in order to determine the crack depth from a single strain measurement.

2.2 Procedure for multiple strain measurements

With the aim to identify the crack surface length as well as the crack depth, a size estimation procedure using multiple strain measurements was developed previously by the author [6]. In this procedure, multiple strains are measured around the cracked portion as schematically shown in Fig. 5. Since the strain depends not only on the crack depth but also on the surface length, possible combinations of the crack depth and surface length can be obtained for each measured strain as schematically shown in Fig. 6. The estimated crack depth depends on the surface length; the crack depth decreases as the surface length increases. In this study, the curve representing the possible combinations of the depth and surface length is referred to as an "ac-curve". The ac-curve is drawn using a data set which is generated by FEAs for various crack shapes. A different ac-curve is obtained at a different position even if the crack geometry is the same. If two ac-curves intersect each other, the point of intersection corresponds to the depth and surface length of the crack. If the number of strain gages is increased, the number of crossing ac-curves as well increases. By taking the average of the crossing points, it is possible to reduce the error in the crack size identification.

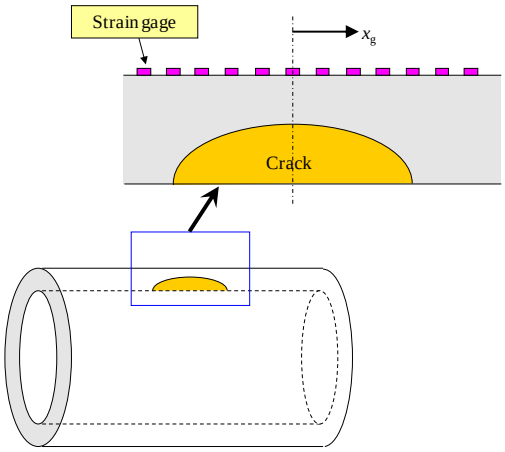

Fig. 5 Multiple strain measurement method for crack growth monitoring.

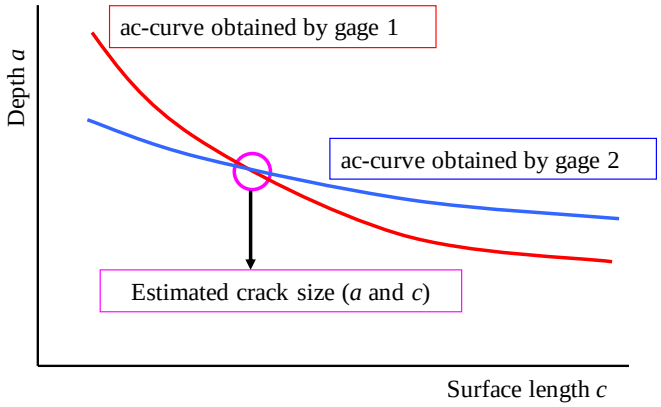

Fig. 6 Schematic of the estimation procedure for the crack depth and surface length from a combination of two strains at different positions.

Table 1 Elemental content (wt %) of pipe

Fe	C	Si	Mn	P	S
Bal.	0.21	0.22	0.80	0.019	0.007

Table 2 Kinds of articles and reviewing process

Yield strength	Tensile strength	Elongation
265 **MPa**	489 **MPa**	0.50

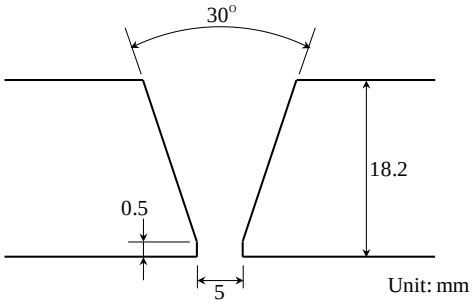

Fig. 7 Geometry of welding groove.

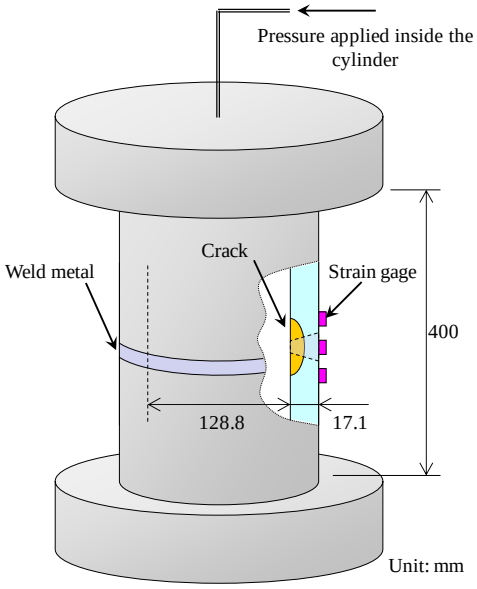

Fig. 8 Schematic of experiment apparatus for fatigue crack growth by cyclic internal pressure.

3 Experiment

3.1 Experimental procedure

Butt-welded pipe was made from a carbon steel pipe (STS370 in JIS). Tables 1 and 2 list the elemental composition and mechanical properties of the pipe. The outer diameter and thickness were 165.2 **mm** and 18.2 **mm**, respectively. The pipe was cut in two pieces at the center in the longitudinal direction and a single V-groove was machined for butt welding as shown in Fig. 7. The pipes were joined by arc welding with tungsten inert gas (TIG). After welding, the outer and inner surfaces including the weld bead were machined off to a uniform thickness of 17.1 **mm** (outer diameter of 163.0 **mm)**.

An axial notch was introduced inside the pipe at the center of the welding line using an electrode discharge machine. The depth and surface length of the notch generated by a semi-circular foil electrode were respectively a_o = 4.71 **mm** and and $2c_o$ = 10.04 **mm**, and the width of the notch was 0.28 **mm**. Blind flanges were attached to both ends of the pipe to maintain the internal pressure. Figure 8 shows a schematic illustration of the experimental setup for the welded and notched pipe.

Figure 9 shows the position of the strain gages attached at the outer surface of the pipe. Three sets of array gages were used. Each array had five bi-axial strain gages. The position of the strain was denoted by a parameter x_g with the maxima (maximum x_g) as 18 **mm**. The strains were measured under a constant internal pressure of 30 **MPa**.

3.2 Experimental results

Changes in the strains during the experiment are shown in Fig. 10 together with the changes in applied pressure. The strain gages for the uncracked position were attached at every 90° in the circumferential direction. Almost identical strains were measured for the uncracked positions. The outside strain was reduced due to the crack, and the hoop strain was larger than the axial strain.

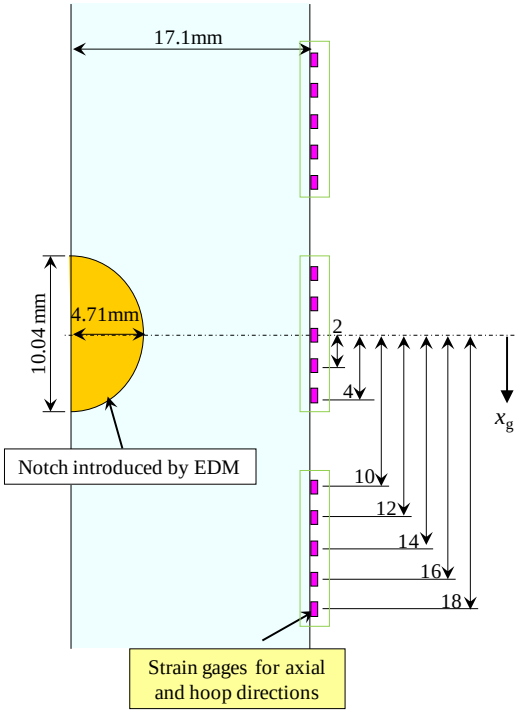

Fig. 9 Positions of strain measurements (unit: **mm**).

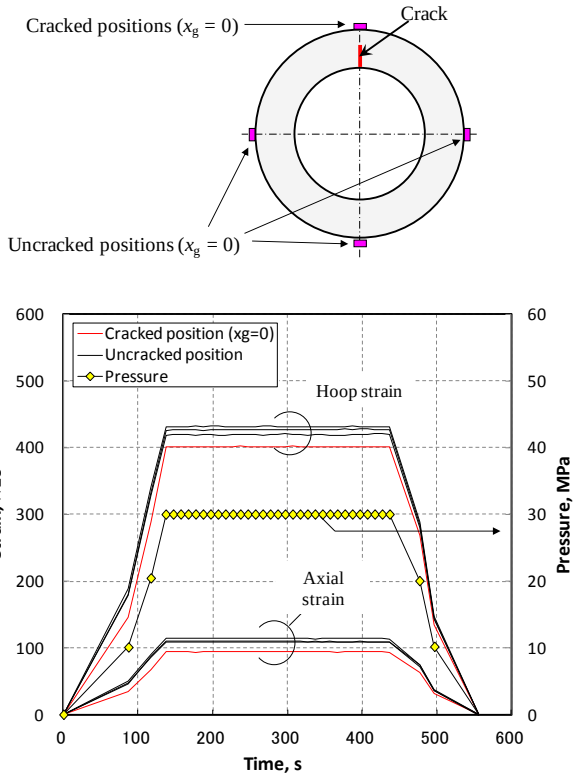

Fig. 10 Measured hoop and axial strains for cracked and uncracked positions (x_g = 0).

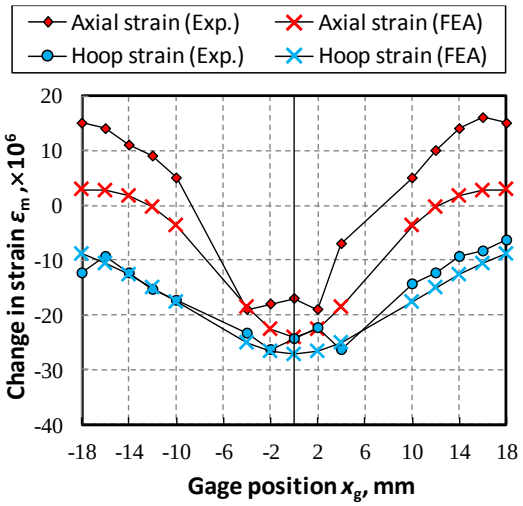

Fig. 11 Strains from measurement (Exp.) and finite element analysis (FEA).

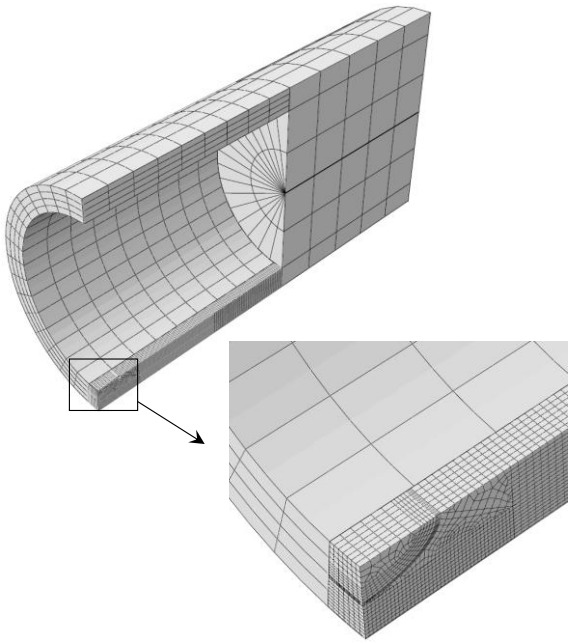

Fig. 12 Finite element meshes for cracked pipe ($a = 0.5t$, $c = t$).

Figure 11 shows the change in strain obtained for each strain gage. The change in strain ε_m was defined by:

$$\varepsilon_m = \varepsilon_{uc} - \varepsilon_c \qquad (1)$$

where ε_c and ε_{uc} denote the strains measured at a cracked and an uncracked position, respectively, measured at the pressure of 30 **MPa**. The average of the three strains has been termed as the strain at the uncracked position. Notable is that the change in strain was relatively small at the crack center

and was not zero within the gage position range of x_g = 18 **mm** to –18 **mm**.

4 Estimation of crack size

4.1 Finite element analysis

FEAs were performed in order to obtain the relationship between crack size and strain distribution outside the pipe. The general-purpose finite element program ABAQUS (Version 6.11) was used for elastic analysis. Figure 12 shows an example of the finite element model for (c/t, a/t) = (1.0, 0.5), consisting of 17,212 20-node isoparametric quadratic solid elements and 82,436 nodes. Due to the symmetries of the model, only one quarter of the cracked pipe was modeled by finite elements. Young's modulus of 206.5 GPa and Poisson's ratio of 0.3 were used as the elastic constants. The material (inclusive of the weld metal) was assumed to be isotropic and homogeneous.

The crack was modeled as semi-circular or semi-elliptical in shape. The crack size was changed by 0.05t from 0.05t to 0.9t in the depth direction, and from 0.2t to 1.5t in the surface direction. FEAs were performed for the possible combinations of the depth and surface length (*viz.* 486 cases).

The internal pressure was applied to the inside pipe including the crack face. The outside strain was derived by extrapolating strains obtained at integration points of the outer element, which had a thickness of 0.01t. The outside strains were stored as a data set for obtaining the ac-curves.

4.2 Estimation using single strain gage

The crack depth was estimated using the hoop or axial strain at x_g = 0. Figure 13 shows the change in strain ε_m obtained by FEAs for the fixed crack surface length of 2c = 10.04 **mm**, which was the measured value. The strain decreased as the crack depth increased, and the crack depth was estimated by comparing the strains obtained by FEAs and by the measurement. The error in estimation obtained by the hoop and axial strains was 0.45 **mm** and 0.75 **mm**, respectively. In order to estimate the crack depth, the surface length has to be assumed. Therefore, the estimation procedure using Fig. 13 is applicable only for limited cases.

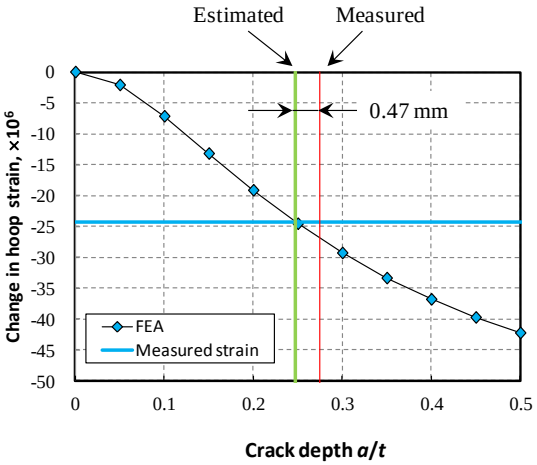

(a) Estimation by hoop strain

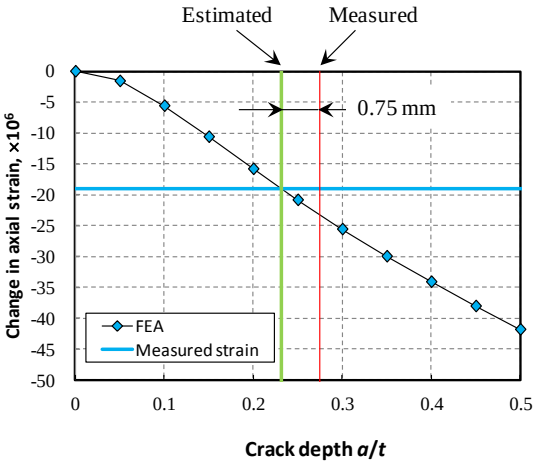

(b) Estimation by axial strain

Fig.13 Crack depth estimation from measured strain. FEA was done for a crack of measured surface length (2c = 10.04 **mm**).

4.3 Estimation using multiple strain gages

The crack size was estimated according to the aforementioned procedure. The ac-curves were derived from measured strains using the data set obtained by FEAs. Figure 14(a) shows the ac-curves (a series of points) obtained. The measured crack size was (c/t, a/t) = (0.30, 0.28). Although, the curves tend to be focused around the crack size, which is indicated by the intersection of the vertical and horizontal blue lines, significant scattering was observed particularly in axial strains. If the crack was assumed to be ideal and semi-elliptical in shape and exact strains were assumed to be measured, the ac-curves would cross at one point as shown in Fig. 14(b). In the case of Fig. 14(a), 30 ac-curves were obtained and the number of crossing points was 33, whereas 337 crossing points were expected from Fig.

14(b). The crack size was estimated from the crossing points of two ac-curves. Figure 15 shows the estimated crack sizes from the crossing points. Although the crossing points show eminent scatter, the average of the points appear to coincide with the experimental result.

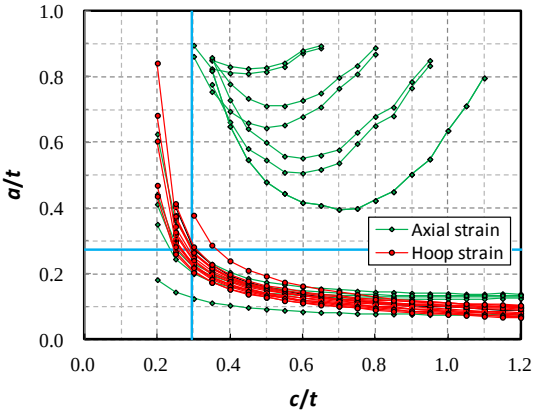

(b) From measured strains

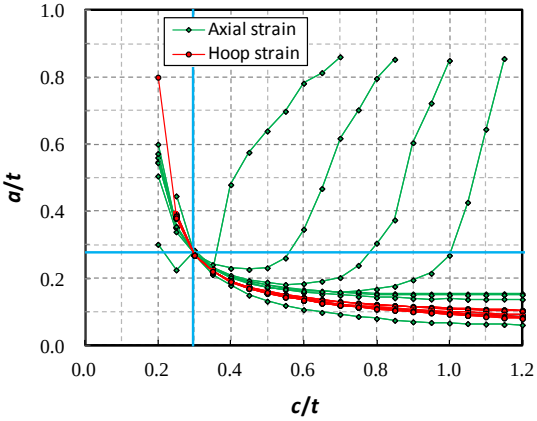

(b) From FEA (corresponding to accurate measurement)

Fig. 14 The ac-curves obtained using measured strains(measured size: c/t = 0.30, a/t = 0.28).

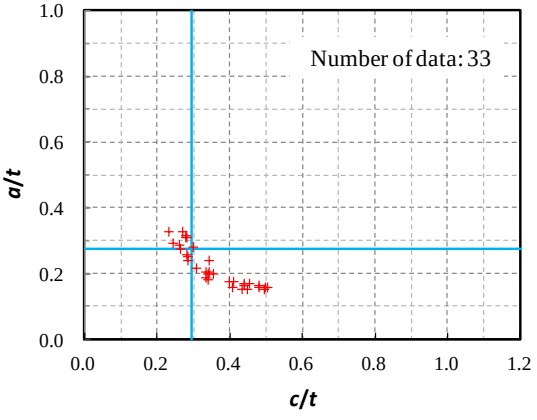

Fig. 15 Crossing points of ac-curves (measured size: c/t = 0.30, a/t = 0.28).

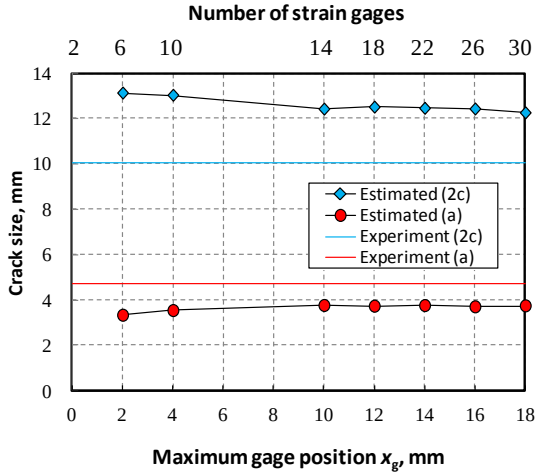

Fig. 16 Change in estimated crack size with the number of strain gages.

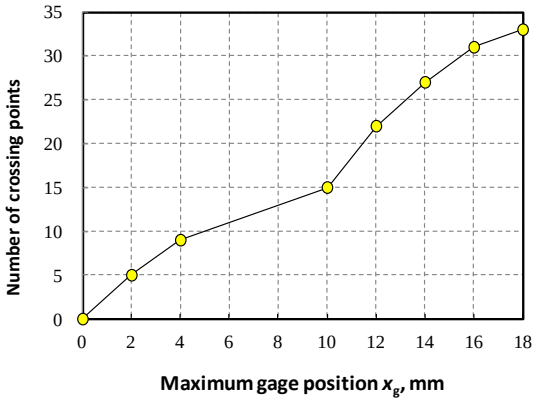

Fig. 17 Change in number of crossing points with the number of strain gages.

The average of the crack sizes obtained from each crossing point was defined as the estimated crack size. The change in the estimated crack size with the number of strain gages is shown in Fig. 16. The strain gages used for the estimation were increased from the crack center. For example, in the case of x_g = 4 **mm**, the strain gages at x_g = 0, ±2and±4 **mm** (10 gages) were used for averaging. The number of crossing points used for the estimation is shown in Fig. 17. The ac-curves for the hoop and axial strains at x_g = 0 did not intersect each other. Therefore, the number of crossing points was zero at x_g = 0. The crossing point increased with the number of strain gages. The accuracy of crack size estimation improved as the number of strain gages increased. The estimated crack size using all gages was $2c$ = 12.25 **mm** and a = 3.74 **mm**, and corresponding error in the estimation were 2.2 **mm** and 0.97 **mm,** respectively.

5 Discussion

The change in strain derived by FEAs is superimposed as is envisaged in Fig. 11. The axial strains showed relatively large deviation from FEA results, while almost identical strains were measured for the hoop strains.

The difference in Young's modulus and Poisson's ratio may cause the difference between the measured strains and FEA results. The anisotropy and inhomogeneity of the material properties also affect the strain. In particular, the weld metal may show a peculiar deformation, although the detailed material properties were not identified in this study. It should be emphasized that the influence of such factors has little effect on the current estimation procedure because the change in strain was used for the size estimation [5]. The difference in material properties between the measurement and FEA was almost canceled by taking the relative strain from the uncracked position.

The residual stress caused by the welding might alter the strains. Since the change in strain was used for the estimation and the strain remained in the elastic region, the influence of the residual stress was deduced to be insignificant. However, the residual stress may affect the strain measurements of operating components because the residual strain is released due to crack growth. When the release of the residual strain is significant, a valid change in strain for size estimation is difficult to obtain from continuous strain measurements. Therefore, for the growth monitoring of cracks initiated at a welded portion, the change in strain free from the influence of released strain has to be identified. For example, an unexpected plant shut down, load change, or change in flow in the piping may cause the strain change without releases of residual strain as simulated in this study.

It should be noted that a crack may not grow during the plant operation. Since the growth rate of macroscopic cracks is relatively fast, it has been deduced that cracks detected by inspections have already ceased growing in most cases [7][8]. Therefore, it is important to show the crack has been dormant from an engineering viewpoint. If the crack does not grow, the change in strain is expected to stay constant regardless of the residual stress.

6 Conclusion

In order to validate the crack growth monitoring method using multiple strain gages, an experiment using a welded carbon steel pipe was conducted. An axial notch was introduced inside the pipe perpendicular to the butt welding line, the change in strains was then measured by applying an internal pressure. The validity and accuracy of the monitoring method were discussed by comparing with the experimental results. The following conclusions were drawn from this study:

a. The monitoring procedure using multiple strain gages could estimate not only the crack depth but also the surface length.
b. The maximum estimation errors were 2.2 **mm** and 0.97 **mm** for the surface length and depth, respectively. The accuracy was improved by increasing the number of strain gages used for the estimation.
c. The residual stress had little effect on the size estimation, although it may have profound effect when the crack propagates.

References

[1] The Japan Society of Mechanical Engineers: Codes for Nuclear Power Generation Facilities, Rules of Fitness-for-Service for Nuclear Power Plants, JSME S NA1-2008: Tokyo, JSME, 2008.

[2] The American Society of Mechanical Engineers: Rules for In-service Inspection of Nuclear Power Plant Components - ASME Boiler and Pressure Vessel Code Section XI, New York: ASME, 2010.

[3] KONO, K., OTAKA, M., MIHARADA, H., SAKAMOTO, K., KOMURA, I., and FURUKAMA, T.: Detectability and Sizing Capability of UT to SCC in Nickel based Alloy Welded Joint, In: Proc. 7th International Conference on NED in Relation to Structural Integrity for Nuclear and Pressurized Components, Yokohama, European Commission JRC, 2009, 360-364.

[4] KAMAYA, M., and MIYOSHI, K.: Crack Growth Monitoring by Strain Measurement of External Surface of Cracked Pipe. In: Proc. 18th International Conference on Nuclear Engineering, Xi'an, ASME, 2010, paper no. 29843.

[5] KAMAYA, M., and MIYOSHI, K.: Monitoring of Inside Surface Crack Growth by Strain Measurement of

the Outside Surface, A feasibility study, Nuclear Engineering and Design, 2011, 241: 1-11.

[6] KAMAYA, M.: Growth Monitoring of Internal Surface Crack by Strain Measurement of External Surface (part I: Development of Multiple Strain Measurement Method), Transactions of the Japan Society of Mechanical Engineers, 2011, 77A: 2001-2011.

[7] TAHERI, S.: Some Advances on Understanding of High Cycle Thermal Fatigue Crazing, Journal of Pressure Vessel Technology, 2007, 129: 400-410.

[8] KAMAYA, M., and TAHERI, S.: A Study on the Evolution of Crack Networks under Thermal Fatigue Loading, Nuclear Engineering and Design, 2008, 238: 2147-2154.